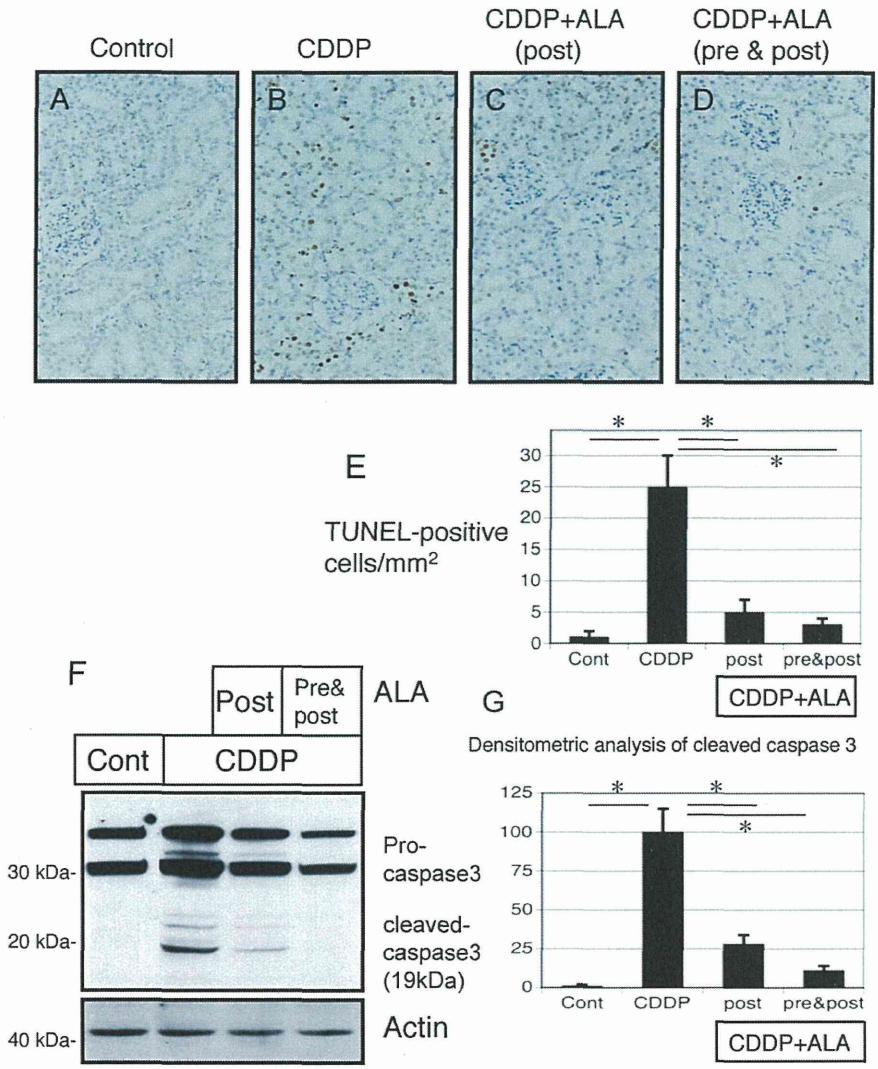

Figure 3. Tubular cell apoptosis and levels of cleaved caspase3 in renal tissues of ALA treated rats with cisplatin-inducedAKI. Kidneys were removed 5 days after an injection with cisplatin (8 mg/kg). A, B) Kidneys of cisplatin-treated rats exhibited an elevated number of TUNEL-positive renal tubular cells. (Magnification, X100). C, D) Kidneys of ALA treatment (both post and pre & post) show a very few number of TUNEL-positive renal tubular cells. (Magnification, X100) E) The number of TUNEL positive tubular cells was significantly low in ALA (both post and pre & post) treated rat kidneys in cisplatin-induced AKI. (F) Western blot analysis of cleaved caspase3 were performed in each group rats. (G) Quantitative densitometry was performed for cleaved caspase 3 blots. Data are the mean ± SEM of 6 rats per group. Statistically significant differences (*$p<0.05$) are indicated.

doi:10.1371/journal.pone.0080850.g003

Cell culture

NRK-52E cells (renal tubular cells from adult rats), originally purchased from American Type Culture Collection, were grown in Dulbecco's modified Eagle's medium (Gibco, Rockville, MD, USA) supplemented with 50 IU/mL penicillin and 10% heat-inactivated fetal calf serum (Gibco) [15]. For the cisplatin experiments, cisplatin (20 μM) was added to the NRK-52E cells for 24 h. For the ALA + cisplatin experiments, 200 μM 5-ALA, 100 μM sodium ferrous citrate, and 20 μM cisplatin were added to the NRK-52E cells for 24 h. All other chemicals were purchased from Funakoshi (Tokyo, Japan).

Isolation and histological examination of kidney tissue

Rats were anesthetized with pentobarbital at the indicated times after cisplatin administration. The kidneys were perfused in situ with sterile phosphate-buffered saline (PBS) and the left kidney was then rapidly excised, frozen in liquid nitrogen, and homogenized in SDS sample buffer, as described previously [16]. For immunohistochemical studies, kidneys were fixed in formalin overnight, dehydrated, and embedded in paraffin. Thin sections were cut and subjected to periodic acid-Schiff staining, as described previously. Tubular injury was assessed by using a semiquantitative scale [6]. Histological changes due to tubular necrosis were quantitated by determining the percentage of tubules with evident cell necrosis, loss of brush border, cast formation, and tubule dilatation, as follows: 0 = none, 1 = ≤10%, 2 = 11%–25%, 3 = 26%–45%, 4 = 46%–75%, and 5 = ≤76%. At least 5–10 fields (×200) were reviewed for each slide. The Apoptosis TUNEL Kit II (MBL, Tokyo, Japan) was used for the staining of terminal deoxynucleotidyl transferase-mediated dUTP nick end labeling (TUNEL)-positive cells, as previously described [6].

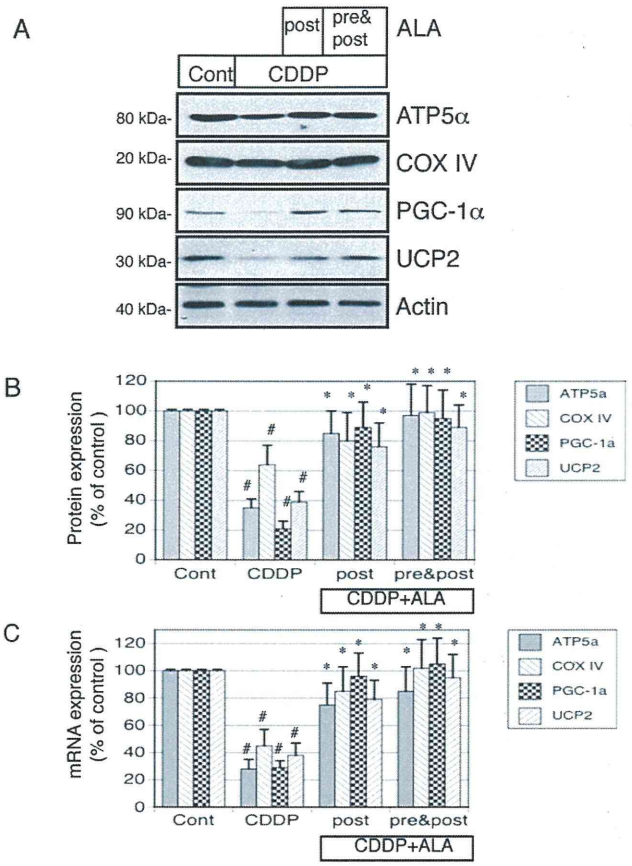

Figure 4. Western blot analyses of protein expression and RT-PCR analysis of mitochondria-related gene expression in ALA treated cisplatin-induced AKI rats. (A) Aliquots of 50 μg of protein from renal tissue extracts were separated by SDS-PAGE and transferred to membranes. Western blots analyses were performed for ATP5α, complex (COX)-IV, PGC-1α, UCP2 in cisplatin-treated, control, and cisplatin + ALA (both post and pre & post) treated rats. Actin served as a loading control. (B) Quantitative densitometry was performed for ATP5α, complex (COX)-IV, PGC-1α, and UCP2 western blots. (C) Quantitative analysis of mRNA was performed using RT-PCR for ATP5α, complex (COX)-IV, PGC-1α, and UCP2. GAPDH served as a loading control. Bars represent the mean ± SEM, n = 6. *$p<0.05$ v.s. CDDP, #$p<0.05$ v.s. control by ANOVA.
doi:10.1371/journal.pone.0080850.g004

Western blot analysis

Protein extracts of the total renal tissue or NRK-52E cells (50 μg samples) were prepared and denatured by heating at 100°C for 5 min in SDS sample buffer as described previously [17]. The proteins were separated on 7.5% or 10%–20% polyacrylamide gels and transferred to nitrocellulose membranes. The membranes were blocked for 1 h with 5% (wt/vol) fat-free milk in PBS and probed with the appropriate primary antibodies (anti-ATP5α, anti-complex [COX]-IV, anti-PGC-1α, anti-UCP2, anti-nitrotyrosine [anti-NT], anti-procaspase-3, or anti-actin [Santa Cruz Biochemicals Inc., Santa Cruz, CA, USA]). The primary antibodies were detected with horseradish peroxidase (HRP)-conjugated rabbit anti-goat IgG or HRP-donkey anti-rabbit IgG, and visualized by using the Amersham ECL system (Amersham Corp., Arlington Heights, IL, USA).

Measurements of heme

We measured heme to evaluate the metabolic product of ALA using assay kit (BioChain Institute, Newark, CA). Heme Assay Kit is based on an improved aqueous alkaline solution method, in which the heme is converted into a uniform colored form. The intensity of color, measured at 400 nm, is directly proportional to the heme concentration in the sample. We measured the renal tissue extract in the in vivo experiments, and the cell extracts in the in vivo experiments. The protein extracts of the total renal tissue or NRK-52E cells (100 μg samples) were prepared following the same method used in the immunoblot analysis.

Real-time quantitative polymerase chain reaction

Reverse transcription-polymerase chain reaction (RT-PCR) analysis of RNA extracted from kidneys was carried out as previously described [16]. In brief, total RNA was isolated from renal tissues by using TRI Reagent (Life Technologies, Gaithersburg, MD, USA). Samples of total RNA (1 μg) were reverse transcribed, and real-time qPCR was performed to quantify changes in *ATP5α*, *COX-IV*, *PGC-1α*, and *UCP2* gene expression by using the ABI LightCycler real-time PCR system (ABI, Los Angeles, CA, USA). RT-PCR of glyceraldehyde-3-phosphate dehydrogenase (GAPDH) served as a positive control. A 3-step PCR was performed for 35 cycles. The samples were denatured at 94°C for 30 s, annealed at 58°C for 30 s, and extended at 72°C for 30 s. The primers were obtained from ABI.

Mitochondrial morphology obtained by using laser confocal immunofluorescence microscopy

NRK-52E cells were stained with MitoTracker mitochondrion-selective probes (Invitrogen, Rockville, MD, USA). For confocal microscopy, NRK-52E cells were then fixed with 2% paraformaldehyde in PBS for 1 h and processed for imaging as described previously, and examined under a confocal laser microscope (Carl Zeiss Japan, Tokyo, Japan) [18]. Fragmented mitochondria were condensed and punctate, whereas normal mitochondria showed a threadlike or rounded structure. Cells with mitochondrial fragmentation were defined as those containing a majority (>70%) of fragmented mitochondria, and they were counted to determine the percentage in 50 cells/sample.

Statistics

Results are presented as mean ± SEM. Differences between the groups were tested by 2-way analysis of variance (ANOVA) followed by Scheffe's test for multiple comparisons. Two groups were compared by using unpaired *t*-tests. A p value of <0.05 was considered statistically significant.

Results

5-Aminolevulinic acid protects from cisplatin-induced renal injury

Cisplatin increased the serum blood urea nitrogen and creatinine levels in comparison with the controls at days 5–9. ALA treatments (both post and pre & post) significantly prevented these changes in cisplatin-treated animals (Figure 1A,B). Body weight was not significantly different in rats before the beginning of the treatment. Cisplatin reduced body weight gain in the test animals. ALA treatments (both post and pre & post) significantly prevented, but did not normalize, cisplatin-induced weight loss (Figure 1C). The toxic effect of cisplatin was also confirmed by the detection of morphologic abnormalities in kidney slices. The histology results for the control rats were normal (Figure 2A). The

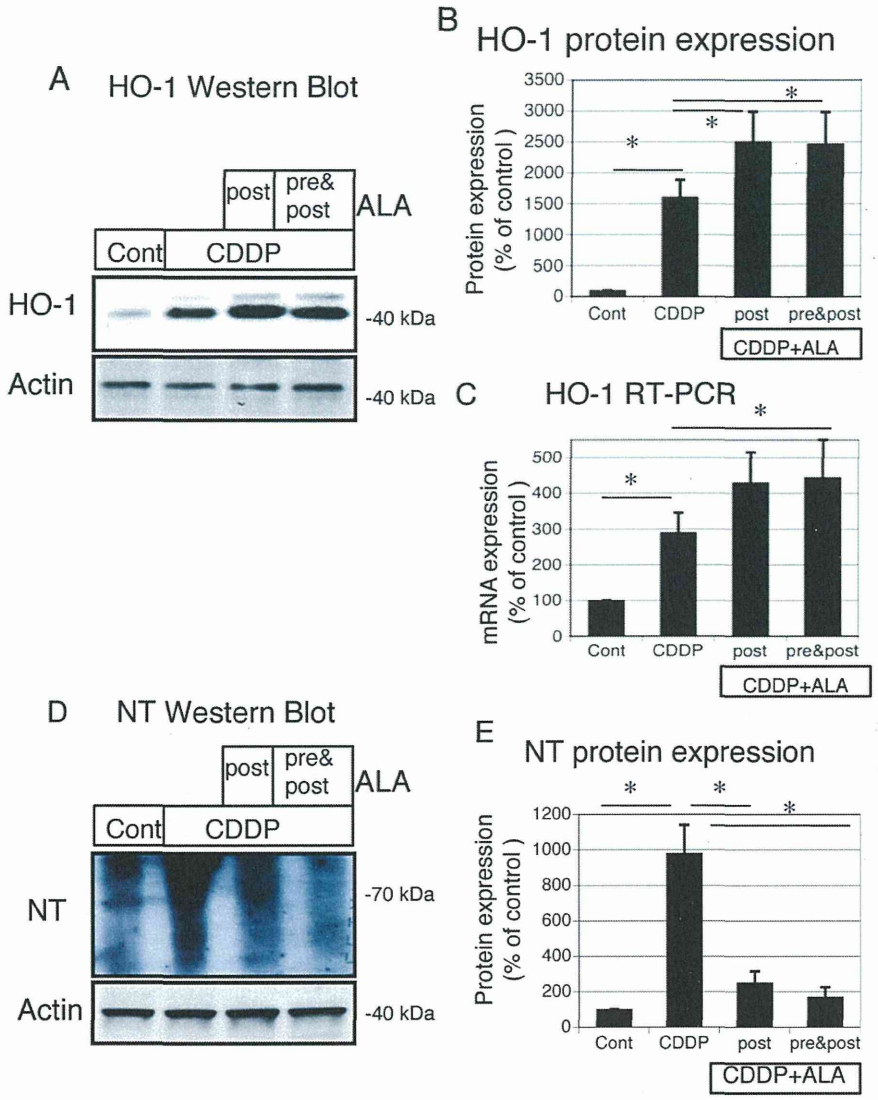

Figure 5. Protective effects of ALA to cisplatin-induced oxidative stress and induction of Heme oxygenase (HO)-1 expression in vivo. (A, D) Aliquots of 50 μg of protein from renal tissue extracts were separated by SDS-PAGE and transferred to membranes. Western blots analyses were performed for HO-1 (A), nitrotyrosine (NT) (D) in cisplatin-treated, control, and cisplatin + ALA (both post and pre & post) treated rats. Actin served as a loading control. (B) Quantitative densitometry was performed for HO-1 western blots. (C) Quantitative analysis of mRNA was performed using RT-PCR for HO-1. GAPDH served as a loading control (E) Quantitative densitometry was performed for NT western blots. Bars represent the mean ± SEM, n = 6. *P<0.05 by ANOVA.
doi:10.1371/journal.pone.0080850.g005

cisplatin group exhibited acute structural damage characterized by tubular necrosis, swelling and tubular dilation, extensive epithelial vacuolization, and hyaline casts in renal tubules (Figure 2B–D). ALA reduced these tubular damages in cisplatin-treated rats (Figure 2C,D). The semiquantitative histological injury score was significantly higher in cisplatin-treated rats than in controls (Figure 2E).

5-Aminolevulinic acid reduces cisplatin-induced apoptosis

Apoptosis in the kidney was assessed by using the TUNEL assay. Cisplatin increased the number of apoptotic nuclei compared with the control group (Figure 3A,B). ALA treatments (both post and pre & post) significantly decreased the number of TUNEL-positive cells (Figure 3C,D). The number of TUNEL-positive cells were increased by cisplatin treatment and reduced by ALA administration (both post and pre & post) on quantitative analysis (Figure 3E). Cleaved caspase-3 levels were high in the renal tissue of rats treated with cisplatin. ALA treatments (both post and pre & post) significantly lowered the elevated caspase-3 levels in cisplatin-injected rat kidneys, as assessed by western blotting of the renal tissue and densitometric analysis (Figure 3F,G).

5-Aminolevulinic acid ameliorates cisplatin-induced reduction of mRNA and protein expression of mitochondria-related genes in vivo

We next examined whether ALA protects the mitochondrial enzymes from cisplatin injury. Because previous studies demonstrated that cisplatin caused a marked decrease in the expression of several mitochondrial enzymes, we examined typical enzymes (ATP5α, COX-IV, PGC-1α, and UCP2) in cisplatin-treated, control, and cisplatin + ALA–treated rats. As shown in Figure 4A,

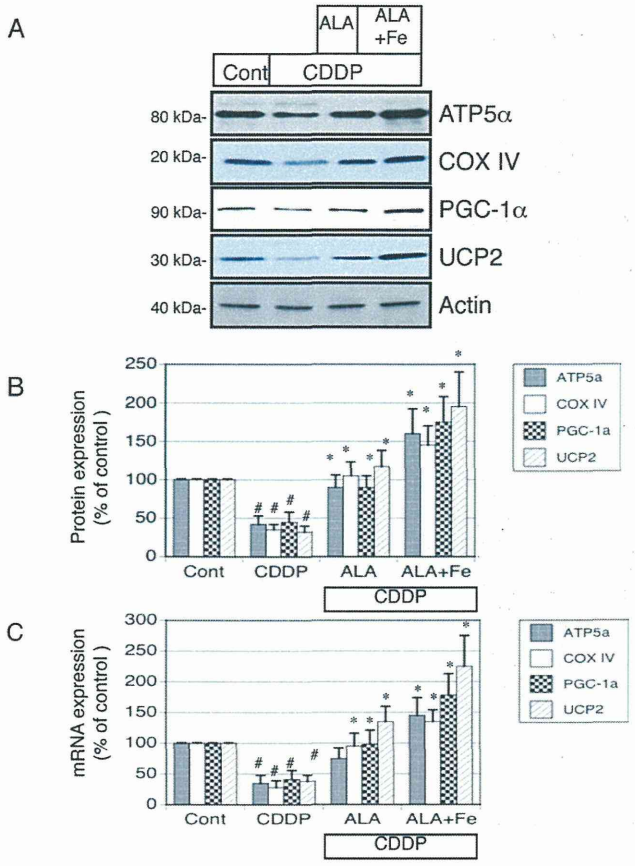

Figure 6. Western blot analyses of protein expression and RT-PCR analysis of mitochondria-related gene expression in ALA + Fe treated cisplatin-induced renal tubular injury. (A) Aliquots of 50 μg of protein extracts from NRK-52E cells were separated by SDS-PAGE and transferred to membranes. Western blots analyses were performed for ATP5α, complex (COX)-IV, PGC-1α, UCP2 in control, cisplatin, cisplatin + ALA, and cisplatin + ALA + Fe treated NRK-52E cells. Actin served as a loading control. (B) Quantitative densitometry was performed for ATP5α, complex (COX)-IV, PGC-1α, and UCP2 blots. (C) Quantitative analysis of mRNA was performed using RT-PCR for ATP5α, complex (COX)-IV, PGC-1α, and UCP2. Bars represent the mean ± SEM, n = 6. *p<0.05 v.s. CDDP, #p<0.05 v.s. control by ANOVA.
doi:10.1371/journal.pone.0080850.g006

cisplatin induced a significant loss of ATP5α, COX-IV, PGC-1α, and UCP2 protein expression. ALA treatment (both post and pre & post) recovered the cisplatin-induced decreases of ATP5α, COX-IV, PGC-1α, and UCP2 protein expression. Quantitative analysis revealed that cisplatin induced decreases of ATP5α, COX-IV, PGC-1α, and UCP2 protein expression, and these reductions were ameliorated by ALA treatments (both pre and pre & post) (Figure 4B). Furthermore, to examine the changes in the expression of these enzymes during cisplatin-induced AKI, we conducted an RT-PCR analysis of rat renal tissue mRNA. The mRNA levels of ATP5α, COX-IV, PGC-1α, and UCP2 were dramatically decreased by cisplatin, and these reductions were ameliorated by ALA treatments (both pre and pre & post) (Figure 4C).

5-Aminolevulinic acid protects against cisplatin-induced oxidative stress and induces heme oxygenase-1 expression in vivo

We next examined the renal HO-1 expression in the 4 groups of rats. HO-1 mRNA and protein expression was induced by cisplatin treatment in vivo (Figure 5A–C). ALA treatments (both post and pre & post) further increased HO-1 expression (Figure 5A–C). Oxidative stress is a major factor causing renal injury in response to cisplatin. We examined the level of oxidative stress by using a typical marker, NT. On immunoblotting, NT was highly expressed in the cisplatin-treated kidney compared with the control (Figure 5D,E). However, treatments with ALA (both post and pre & post) reduced these signals (Figure 5D,E). These data suggest that cisplatin induced oxidative stress in damaged tubules, whereas such stress was significantly blocked by the ALA treatment.

5-Aminolevulinic acid and Fe protect against cisplatin-induced reduction of mRNA and protein expression of mitochondria-related genes in NRK-52E cells

We next examined whether ALA and Fe protect the mitochondrial enzymes from cisplatin injury in vitro. We examined the typical enzymes (ATP5α, COX-IV, PGC-1α, and UCP2) in the control, cisplatin-, cisplatin + ALA-, and cisplatin + ALA + Fe–treated NRK-52E cells. As shown in Figure 6A,B, cisplatin induced a significant loss of ATP5α, COX-IV, PGC-1α, and UCP2 protein expression. ALA-, and ALA + Fe–treatment completely recovered the cisplatin-induced decreases in the expression of these proteins. Furthermore, to examine the changes in the mRNA expression of ATP5α, COX-IV, PGC-1α, and UCP2 after cisplatin treatment, we conducted RT-PCR analysis of mRNA in NRK-42E cells. The mRNA level of these enzymes was dramatically decreased by cisplatin, and these reductions were ameliorated by addition with ALA and, more effectively, ALA + Fe (Figure 6C).

ALA and Fe protect against cisplatin-induced oxidative stress and induce HO-1 expression in NRK-52E cells

We next examined the HO-1 expression in the presence of cisplatin, ALA, and Fe. HO-1 mRNA and protein expression was induced by cisplatin treatment in NRK-52E cells. ALA treatment additionally increased HO-1 expression. ALA + Fe treatment significantly upregulated HO-1 expression in the presence of cisplatin (Figure 7A–C). Oxidative stress is a major factor causing renal injury in response to cisplatin. On immunoblotting, NT was highly induced by cisplatin treatment compared with the control. Treatment with ALA and Fe significantly reduced these signals (Figure 7D,E).

ALA and Fe prevent cisplatin-induced damage of mitochondrial structure and apoptosis in NRK-52E cells

We examined the effects of ALA and Fe on mitochondrial structure by using a laser-scanning confocal microscope. The typical reticulotubular appearance of mitochondria in healthy NRK-52E cells (Figure 8A) had disintegrated into condensed rounded organelles in response to cisplatin at 12 h (arrows in Figure 8B). However, ALA and Fe treatment prevented these structural changes in mitochondria (Figure 8D,E). ALA-only treatment partially prevented these structural changes in mitochondria (Figure 8C,E). We also examined the effects of ALA and Fe in cisplatin-induced apoptosis in NRK-53E cells. We used TUNEL staining to evaluate apoptosis in NRK-52E cells, and found that cisplatin-induced apoptosis was significantly reduced by ALA and ALA + Fe (Figure 9A,B). These data are in accordance with the results of western blot analysis of cleaved caspase-3 (Figure 9C,D).

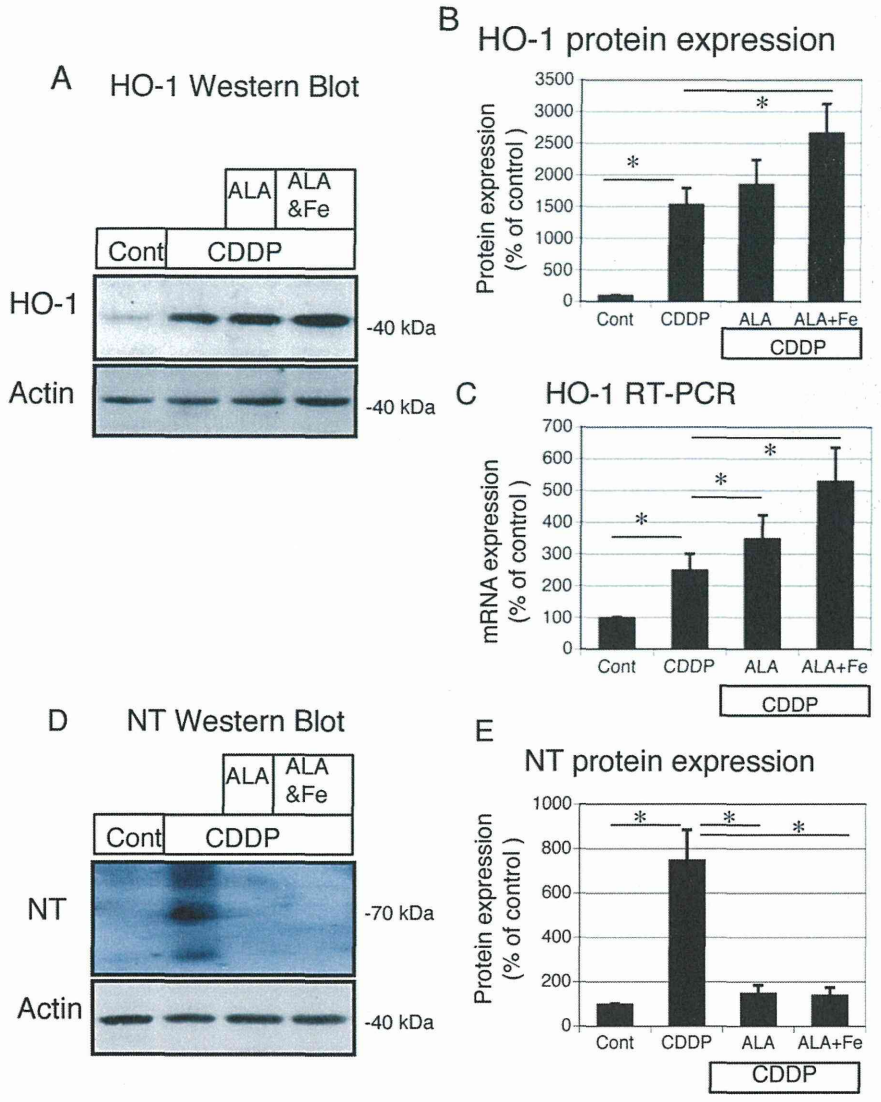

Figure 7. Protective effects of ALA + Fe to cisplatin-induced oxidative stress and induction of Heme oxygenase (HO)-1 expression in NRK-52E cells. (A, D) Aliquots of 50 μg of protein extracts from NRK-52E cells were separated by SDS-PAGE and transferred to membranes. Western blots analyses were performed for HO-1 (A), nitrotyrosine (NT) (D) in control, cisplatin, cisplatin + ALA, and cisplatin + ALA + Fe treated NRK-52E cells. Actin served as a loading control. (B) Quantitative densitometry was performed for HO-1 blots. (C) Quantitative analysis of mRNA was performed using RT-PCR for HO-1. (E) Quantitative densitometry was performed for NT blots. Bars represent the mean ± SEM, n = 6. *P<0.05 by ANOVA.
doi:10.1371/journal.pone.0080850.g007

Measurement of heme in ALA-treated, cisplatin-induced AKI rats and NRK-52E cells exposed to cisplatin and ALA + Fe

We used a heme assay kit to evaluate the metabolic products of ALA. We examined the heme concentration in the renal tissues in the cisplatin-treated, control, and cisplatin + ALA-treated rats. As shown in Figure 10A, cisplatin did not significantly change the heme concentration. ALA treatment (both post and pre + post) significantly increased the heme concentration. We then examined whether ALA and Fe increased heme concentration in vitro. We measured the heme concentrations in the control, cisplatin-, cisplatin + ALA-, and cisplatin + ALA + Fe-treated NRK-52E cells. As shown in Figure 10, cisplatin did not change the heme concentration. ALA as well as ALA + Fe treatment significantly increased the heme concentration. These data demonstrated that heme is up-regulated by ALA treatment both in vitro and in vivo.

Effects of 5-Aminolevulinic acid on the antitumorigenic effects of cisplatin in vivo

To evaluate if the ALA reduction of cisplatin nephrotoxicity was specific for the kidney, we looked for potential reductions in the chemotherapeutic efficacy of cisplatin in bladder carcinoma cells. We evaluated the size of the renal carcinoma transplanted into the rat skin, as shown in Figure 11, and found that cisplatin reduced the size. ALA (post and pre & post) did not change the anticancer effects of cisplatin.

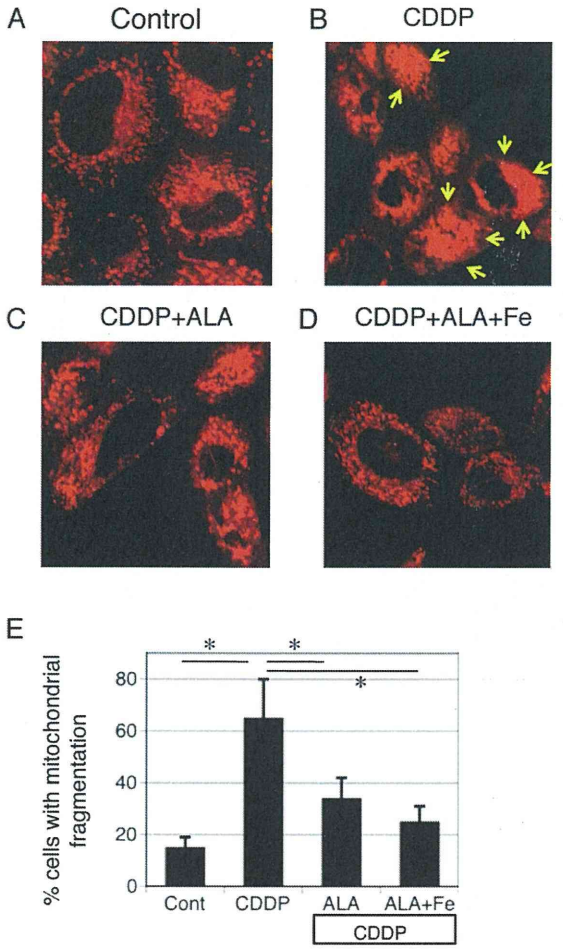

Figure 8. ALA and Fe prevent cisplatin-induced damage of mitochondrial structure in NRK-52E cells. (A–D) Confocal microscopy demonstrates mitochondria structure in NRK-52E cells transfected with mitochondria-targeted red fluorescent protein (mitoDsRed) vectors. NRK-52E cells were treated with in control condition, cisplatin, cisplatin + ALA, and cisplatin + ALA + Fe. Typical condensed rounded organelles in response to cisplatin were marked by arrows. (E) Quantitative analysis of the typical reticulotubular appearance of mitochondria in healthy NRK-52E cells and multiple rounded organelles are performed. ALA and Fe treatment prevented these structural changes in mitochondria. ALA only treatment partially prevented these structural changes in mitochondria. Bars represent the mean ± SEM, n = 6. *P<0.05 by ANOVA.
doi:10.1371/journal.pone.0080850.g008

Discussion

In this study, we demonstrated that the protective role of ALA in cisplatin-induced AKI is through the protection of mitochondrial viability, and ALA prevents tubular apoptosis. In addition, ALA has no significant effects on the anticancer efficiency of cisplatin in rats. Thus, ALA has the potential to prevent cisplatin nephrotoxicity without compromising the anticancer efficacy of cisplatin. Cisplatin is a chemotherapeutic agent that is used in the treatment of a variety of solid-organ cancers, including those of the head, neck, testis, ovary, and breast [19]. Unfortunately, in addition to causing bone marrow suppression, ototoxicity, and anaphylaxis, around 30% of patients receiving cisplatin develop AKI owing to its preferential accumulation within the proximal tubule cells in the outer medulla of the kidney [20,21]. The cellular events in cisplatin-mediated nephrotoxicity, including decreased protein synthesis, membrane peroxidation, mitochondrial dysfunction, and DNA injury, are a consequence of free radical generation and the body's inability to scavenge such molecules [22,23]. Consistent with previous studies, we found that cisplatin-induced renal dysfunction and morphological changes were associated with mitochondrial injury in the rat kidney [9]. These findings were also confirmed by using NRK-52E cells, in which we documented that cisplatin caused mitochondrial fragmentation and decrease of mitochondrial enzymes.

In animal cells, ALA is formed from glycine and succinyl CoA by ALA synthase in mitochondria. COX and cytochrome *c* are hemoproteins. In this study, we demonstrated that COX-IV expression was increased by ALA administration in vivo and in vitro. This finding is in accordance with previous report with liver lysates [24]. ALA is the precursor of protoporphyrin, and heme is produced by the insertion of iron. Therefore, ALA administration can result in heme production in the rat kidney, and it is possible that COX-IV was increased by ALA administration. ALA administration upregulates HO-1 expression. HO-1 is a key enzyme for antioxidant response in renal tubular cells and therefore protects mitochondrial function and upregulates mitochondrial enzymes. We first demonstrated that typical mitochondrial enzymes, such as PGC-1α, UCP2, and ATP5α, were upregulated by ALA administration. Interestingly, ALA and Fe strongly induced these enzymes.

This is the first study to demonstrate that HO-1 is upregulated by ALA and Fe in vivo and in vitro. HO-1 a microsomal enzyme involved in the degradation of heme, resulting in the generation of biliverdin, iron, and carbon monoxide. Recent attention has focused on the biological effects of product(s) of this enzymatic reaction that have important antioxidant, anti-inflammatory, and cytoprotective functions [25]. Induction of HO-1 occurs as an adaptive and beneficial response to a wide variety of oxidant stimuli, including heme, hydrogen peroxide, cytokines, growth factors, heavy metals, nitric oxide, and oxidized LDL [25]. HO-1, the enzyme that is responsible for heme degradation, is upregulated in the proximal tubule cells in response to oxidant stress [26], and once induced, it confers dramatic cytoprotective and anti-inflammatory effects [25,27]. The mechanisms of HO-1 regulation are reported by several pathways: one is hypoxia and inflammatory signals, including IL-1 and TNFα, and second are the nuclear factor E2-related factor-2 (Nrf2) and heme levels. HO-1 gene regulation is reported to involve Kelch-like enoyl-CoA hydratase (ECH)-associated protein 1 (Keap1) regulation through antioxidant response elements (ARE), Nrf2, and their binding in the cytosol [28]. Recently, investigators identified a heme-dependent degradation system involving iron regulatory protein 2 (IRP2) as a sensor of iron metabolism. IRP2 upregulates intracellular free iron and modulates intracellular iron stores, and increased iron efflux has been suggested as a mechanism for the cytoprotective effects of HO-1 expression [29]. We clearly demonstrated that cisplatin itself upregulates HO-1 expression; these findings were in accordance with those of the previous reports [30,31]. Furthermore, we demonstrated that ALA induced HO-1 and ALA + Fe additively upregulated HO-1 mRNA and protein expression in NRK-52E cells. The additional induction of HO-1 by Fe may confer cytoprotective and antioxidant responses in renal tubular cells and protect mitochondrial function and enzymes such as PGC-1α, ATP5α, and UCP2. However, further studies are needed to completely clarify the mechanisms of heme regulation and their associated metabolic pathways concerning mitochondrial function.

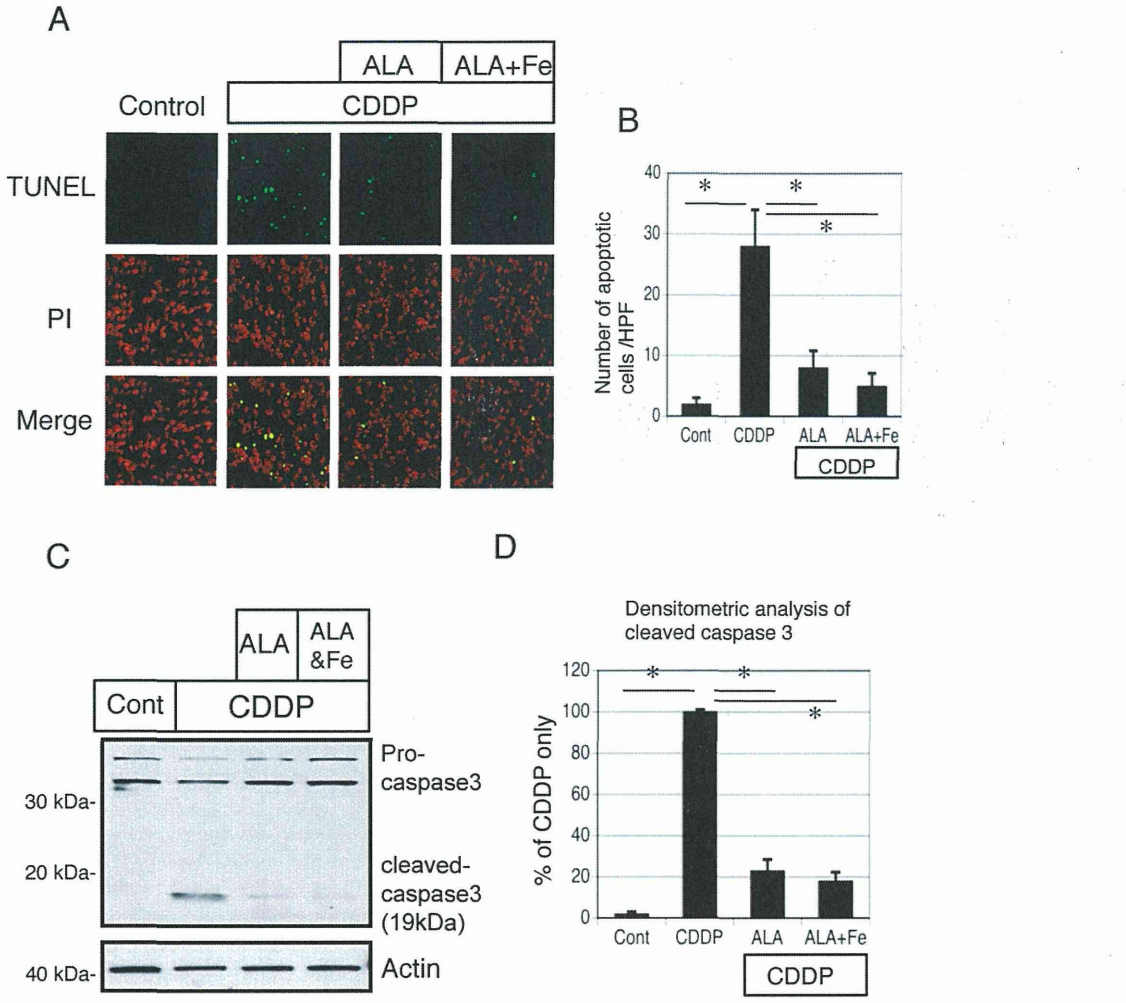

Figure 9. TUNEL assay and cleaved caspase 3 to evaluate apoptosis in NRK-52E cells exposed to cisplatin and ALA + Fe. (A) TUNEL assay to evaluate apoptosis (green) in NRK-52E cells exposed to cisplatin or control. Nuclei were stained with propidium iodide (PI) (red). TUNEL assay to evaluate apoptosis (green) in NRK-52E cells exposed to cisplatin + ALA or cisplatin + ALA + Fe. (B)The induction of the number of apoptotic cells by cisplatin was reduced by ALA and ALA + Fe using quantitative analysis. Data are presented as mean ± SEM, n = 6. *P<0.05 vs. pcDNA-transfected cells. (C) Western blot analysis of cleaved caspase3 were performed following incubation with in control condition, cisplatin, cisplatin + ALA, and cisplatin + ALA + Fe. (D) Quantitative densitometry was performed for cleaved caspase 3 blots. Data are presented as mean ± SEM, n = 6. *P<0.05 by ANOVA.
doi:10.1371/journal.pone.0080850.g009

No previous studies before ours have demonstrated the protective effects of ALA against cisplatin-induced apoptosis in vivo and in vitro. Cisplatin induces apoptosis of renal proximal tubule cells (LLC-PK1) in vitro through mitochondria-dependent and -independent pathways [3], partly through the activation of caspase-3 and oxidative stress [4,5]. Several studies suggest that caspase inhibitors or knockout of apoptosis-related genes attenuate ischemia-induced AKI in rats [32]. In our experiments, cisplatin administration induced apoptosis in vivo and vitro, as confirmed by TUNEL staining and cleaved caspase-3 level. Our data clearly demonstrated that ALA inhibited cisplatin-induced apoptosis in vivo and vitro, which was evaluated by examining the results of TUNEL staining and cleaved caspase-3 levels. Furthermore, ALA + Fe additionally reduced cisplatin-induced apoptosis in NRK-52E cells. The plausible mechanisms of the ALA + Fe effects on antiapoptosis are antioxidative effects and protective effects toward mitochondria in renal tubular cells. In cancer cells, several studies suggested that ALA induces apoptosis through the accumulation of PpIX. ALA-mediated accumulation of PpIX causes photosensitization of cancer cells and is used in the treatment of hepatocellular carcinoma, oral cancer, and bladder carcinoma [13,33]. In several cancer cell lines, ABCG2 transporter is highly expressed and PpIX is accumulated in the cytosol and causes cytotoxic damage and apoptosis [10]. The mechanisms of the differential effects of ALA in the apoptotic pathway in normal renal tubular cells and carcinoma cells are not well known and need to be studied in future.

Cisplatin is one of the most effective and potent anticancer drugs in the treatment of epithelial malignancies [1]. Considering the clinical use of ALA in preventing cisplatin-induced nephrotoxicity, it should be checked whether ALA interferes with the anticancer effects of cisplatin. Thus, we examined the effects of ALA on the size of the renal carcinoma transplanted into rat skin. As shown in Figure 10, cisplatin reduced the size of the

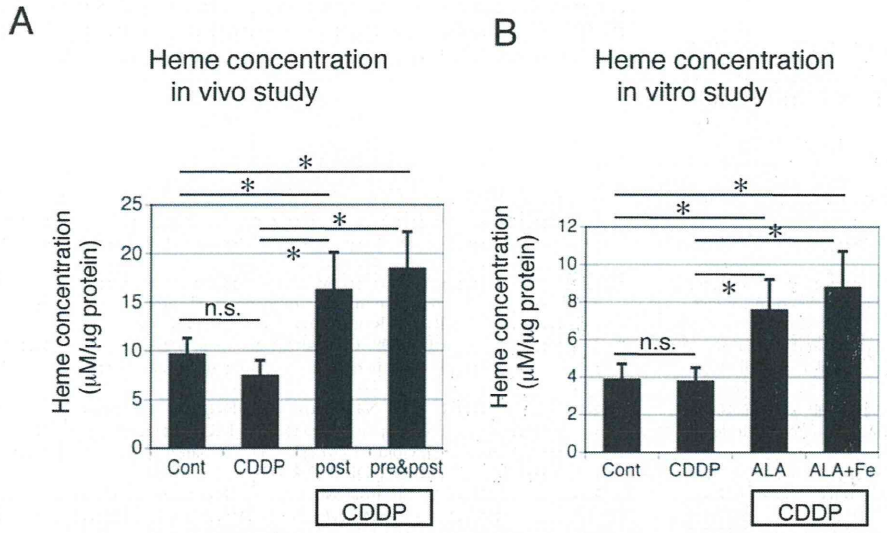

Figure 10. Measurement of heme in the ALA-treated cisplatin-induced AKI rats and NRK-52E cells exposed to cisplatin and ALA + Fe. (A) Aliquots (100 μg) of protein from renal tissue extracts were used for the heme assay in cisplatin-treated, control, and cisplatin + ALA (both post and pre + post)- treated rats. (B) Aliquots (10 μg) of protein extracts from NRK-52E cells were used for the heme assay in the control as well as the cisplatin-, cisplatin + ALA-, and cisplatin + ALA + Fe-treated NRK-52E cells. Data are the mean ± SEM of six experiments per group. *P<0.05 v.s. control or CDDP, n.s. is not significant by ANOVA.
doi:10.1371/journal.pone.0080850.g010

transplanted renal carcinoma. ALA (post and pre & post) did not change the anticancer effects of cisplatin. At least in our experimental condition, ALA did not interfere with the anti-tumorigenic effects of cisplatin in vivo. Further research is needed to gain insight into the effects of ALA on the anticancer effects of cisplatin before clinical use.

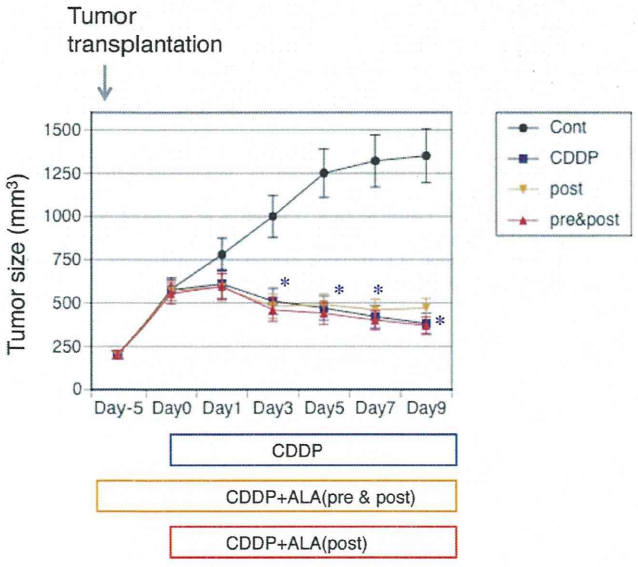

Figure 11. Effects of ALA on anti-tumorinogenic effects of cisplatin in vivo. We evaluated the size of transplantated bladder carcinoma to the F344/NJcl-rnu/rnu rats skin. Rats were divided into four subgroups: 1) a control (saline) group, 2) a cisplatin group, 3) an ALA–treated post cisplatin-injection group, 4) an ALA–treated pre & post cisplatin-injection group (n = 5 for each group), The diameter of the carcinoma were measured at 1, 3. 5, 7, and 9 days after surgery (n = 5/group). Cisplatin reduced size of transplantated renal carcinoma compared with control group. ALA (post and pre & post) did not change the anti cancer effects of cisplatin. Data are the mean ± SEM of 6 experiments per group. *P<0.05 v.s. control by ANOVA.
doi:10.1371/journal.pone.0080850.g011

In summary, our study has produced 2 novel findings. First, the protective role of ALA in cisplatin-induced AKI is through the protection of mitochondrial viability, induction of HO-1, and prevention of tubular apoptosis. Second, ALA has no significant effects on the anticancer efficiency of cisplatin in rats and prevents tubular apoptosis. Further studies are necessary to gain a more precise understanding of the molecular mechanisms by which ALA protects renal cells against cisplatin-induced nephrotoxicity.

Supporting Information

Figure S1 Experimental designs for in vivo study. The rats were given a single intraperitoneal injection of either a vehicle (saline) or cisplatin (8 mg/kg body weight). 5-Aminolevulinic acid (ALA) 10 mg/kg + Fe (sodium ferrous citrate 15.7 mg/kg) were dissolved in drinking water (10 ml/kg) were administered. Rats were divided into four subgroups: 1) a control (saline) group, 2) a cisplatin group, 3) an ALA–treated post (0–9 days after CDDP injection) cisplatin-injection group, 4) an ALA–treated pre(5 days before CDDP injection) & post cisplatin-injection group (n = 8 for each group). Blood samples were obtained for measurement of blood urea nitrogen and serum creatinine. at 1, 3. 5, 7, and 9 days after CDDP injection. Rats were sacrificed at day 5 and 9, and renal tissue are obtained.
(TIF)

Acknowledgments

We thank Ms. Chiaki Kawada, Ms. Reiko Matsumoto, Ms. Sekie Saito, Ms. Akiko Takano, Mr. Yasushi Okada, Ms. Yoko Akimaru, and Mr. Tomomi Anma for technical assistances. We thank Dr. Tohru Tanaka, Dr. Motowo Nakajima, Dr. Atsuko Kamiya, Dr. Kyoko Tsuchiya (SBI Pharmaceuticals Co., Ltd., Tokyo, Japan) for kindly providing sodium ferrous citrate and for helpful discussions.

Author Contributions

Conceived and designed the experiments: Y. Terada Keiji Inoue MT, TS. Performed the experiments: Y. Terada Keiji Inoue TM MI KH YS KO Kosuke Inoue Y. Taniguchi TH TK KT HF SF MT. Analyzed the data: Y. Terada Keiji Inoue TM MI KH YS TK KT HF SF MT. Contributed reagents/materials/analysis tools: Y. Terada Keiji Inoue MT TS. Wrote the paper: Y. Terada Keiji Inoue TS.

References

1. Boulikas T, Vougiouka M (2003) Cisplatin and platinum drugs at the molecular level. (Review). Oncol Rep 10: 1663–1682.
2. Arany I, Safirstein RL (2003) Cisplatin nephrotoxicity. Semin Nephrol 23: 460–464.
3. Park MS, De Leon M, Devarajan P (2002) Cisplatin induces apoptosis in LLC-PK1 cells via activation of mitochondrial pathways. J Am Soc Nephrol 13: 858–865.
4. Kaushal GP, Kaushal V, Hong X, Shah SV (2001) Role and regulation of activation of caspases in cisplatin-induced injury to renal tubular epithelial cells. Kidney Int 60: 1726–1736.
5. Zhou H, Miyaji T, Kato A, Fujigaki Y, Sano K, et al. (1999) Attenuation of cisplatin-induced acute renal failure is associated with less apoptotic cell death. J Lab Clin Med 134: 649–658.
6. Kuwana H, Terada Y, Kobayashi T, Okado T, Penninger JM, et al. (2008) The phosphoinositide-3 kinase gamma-Akt pathway mediates renal tubular injury in cisplatin nephrotoxicity. Kidney Int 73: 430–445.
7. Terada Y, Inoshita S, Kuwana H, Kobayashi T, Okado T, et al. (2007) Important role of apoptosis signal-regulating kinase 1 in ischemic acute kidney injury. Biochem Biophys Res Commun 364: 1043–1049.
8. Hall AM, Rhodes GJ, Sandoval RM, Corridon PR, Molitoris BA (2013) In vivo multiphoton imaging of mitochondrial structure and function during acute kidney injury. Kidney Int 83: 72–83.
9. Ishihara M, Urushido M, Hamada K, Matsumoto T, Shimamura Y, et al. (2013) Sestrin2 and BNIP3 (Bcl-2/adenovirus E1B 19kDa-interacting protein3) regulate autophagy and mitophagy in renal tubular cells in acute kidney injury. Am J Physiol Renal Physiol 305: F495–509 .
10. Kobuchi H, Moriya K, Ogino T, Fujita H, Inoue K, et al. (2012) Mitochondrial localization of ABC transporter ABCG2 and its function in 5-aminolevulinic acid-mediated protoporphyrin IX accumulation. PloS one 7: e50082.
11. Wallin A, Zhang G, Jones TW, Jaken S, Stevens JL (1992) Mechanism of the nephrogenic repair response. Studies on proliferation and vimentin expression after 35S-1,2-dichlorovinyl-L-cysteine nephrotoxicity in vivo and in cultured proximal tubule epithelial cells. Lab Invest 66: 474–484.
12. Inoue K, Kuwana H, Shimamura Y, Ogata K, Taniguchi Y, et al. (2010) Cisplatin-induced macroautophagy occurs prior to apoptosis in proximal tubules in vivo. Clin Exp Nephrol 14: 112–122.
13. Ishizuka M, Abe F, Sano Y, Takahashi K, Inoue K, et al. (2011) Novel development of 5-aminolevurinic acid (ALA) in cancer diagnoses and therapy. Int Immunopharmacol 11: 358–365.
14. Terada Y, Tanaka H, Okado T, Shimamura H, Inoshita S, et al. (2003) Expression and function of the developmental gene Wnt-4 during experimental acute renal failure in rats. J Am Soc Nephrol 14: 1223–1233.
15. Tanaka H, Terada Y, Kobayashi T, Okado T, Inoshita S, et al. (2004) Expression and function of Ets-1 during experimental acute renal failure in rats. J Am Soc Nephrol 15: 3083–3092.
16. Kobayashi T, Terada Y, Kuwana H, Tanaka H, Okado T, et al. (2008) Expression and function of the Delta-1/Notch-2/Hes-1 pathway during experimental acute kidney injury. Kidney Int 73: 1240–1250.
17. Terada Y, Tomita K, Homma MK, Nonoguchi H, Yang T, et al. (1994) Sequential activation of Raf-1 kinase, mitogen-activated protein (MAP) kinase kinase, MAP kinase, and S6 kinase by hyperosmolality in renal cells. J Biol Chem 269: 31296–31301.
18. Tanabe K, Tamura Y, Lanaspa MA, Miyazaki M, Suzuki N, et al. (2012) Epicatechin limits renal injury by mitochondrial protection in cisplatin nephropathy. Am J Physiol Renal Physiol 303: F1264–1274.
19. Lebwohl D, Canetta R (1998) Clinical development of platinum complexes in cancer therapy: an historical perspective and an update. Eur J Cancer 34: 1522–1534.
20. Ries F, Klastersky J (1986) Nephrotoxicity induced by cancer chemotherapy with special emphasis on cisplatin toxicity. Am J Kidney Dis 8: 368–379.
21. Safirstein R, Winston J, Goldstein M, Moel D, Dikman S, et al. (1986) Cisplatin nephrotoxicity. Am J Kidney Dis 8: 356–367.
22. Brady HR, Kone BC, Stromski ME, Zeidel ML, Giebisch G, et al. (1990) Mitochondrial injury: an early event in cisplatin toxicity to renal proximal tubules. Am J Physiol 258: F1181–1187.
23. Lau AH (1999) Apoptosis induced by cisplatin nephrotoxic injury. Kidney Int 56: 1295–1298.
24. Ogura S-I, Maruyama K, Hagiya Y, Sugiyama Y, Tsuchiya K, et al. (2011) The effect of 5-aminolevulinic acid on cytochrome c oxidase activity in mouse liver. BMC Res Notes 4: 66.
25. Agarwal A, Nick HS (2000) Renal response to tissue injury: lessons from heme oxygenase-1 GeneAblation and expression. J Am Soc Nephrol 11: 965–973.
26. Nath KA, Balla G, Vercellotti GM, Balla J, Jacob HS, et al. (1992) Induction of heme oxygenase is a rapid, protective response in rhabdomyolysis in the rat. J Clin Invest 90: 267–270.
27. Nath KA (2006) Heme oxygenase-1: a provenance for cytoprotective pathways in the kidney and other tissues. Kidney Int 70: 432–443.
28. Abraham NG, Kappas A (2008) Pharmacological and clinical aspects of heme oxygenase. Pharmacol Rev 60: 79–127.
29. Ferris CD, Jaffrey SR, Sawa A, Takahashi M, Brady SD, et al. (1999) Haem oxygenase-1 prevents cell death by regulating cellular iron. Nat Cell Biol 1: 152–157.
30. Shiraishi F, Curtis LM, Truong L, Poss K, Visner GA, et al. (2000) Heme oxygenase-1 gene ablation or expression modulates cisplatin-induced renal tubular apoptosis. Am J Physiol Renal Physiol 278: F726–736.
31. Salahudeen AA, Jenkins JK, Huang H, Ndebele K, Salahudeen AK (2001) Overexpression of heme oxygenase protects renal tubular cells against cold storage injury: studies using hemin induction and HO-1 gene transfer. Transplantation 72: 1498–1504.
32. Daemen MA, van't Veer C, Denecker G, Heemskerk VH, Wolfs TG, et al. (1999) Inhibition of apoptosis induced by ischemia-reperfusion prevents inflammation. J Clin Invest 104: 541–549.
33. Hagiya Y, Adachi T, Ogura S, An R, Tamura A, et al. (2008) Nrf2-dependent induction of human ABC transporter ABCG2 and heme oxygenase-1 in HepG2 cells by photoactivation of porphyrins: biochemical implications for cancer cell response to photodynamic therapy. J Exp Ther Oncol 7: 153–167.

Clin Exp Nephrol (2013) 17:848–856
DOI 10.1007/s10157-013-0803-y

ORIGINAL ARTICLE

Serum level of soluble (pro)renin receptor is modulated in chronic kidney disease

Kazu Hamada · Yoshinori Taniguchi · Yoshiko Shimamura · Kosuke Inoue · Koji Ogata · Masayuki Ishihara · Taro Horino · Shimpei Fujimoto · Takashi Ohguro · Yukio Yoshimoto · Mika Ikebe · Kenji Yuasa · Eri Hoshino · Tatsuo Iiyama · Atsuhiro Ichihara · Yoshio Terada

Received: 5 December 2012 / Accepted: 6 March 2013 / Published online: 6 April 2013

Abstract
Background Prorenin, the precursor of renin, binds to the (pro)renin receptor [(P)RR] and triggers intracellular signaling. The ligand binding sites of (P)RR are disconnected and are present in the soluble form of the receptor in serum. Given that the clinical significance of serum prorenin and soluble (P)RR in chronic kidney disease (CKD) is unclear, we investigated the relationship between serum prorenin, soluble (P)RR, and various clinical parameters in patients with CKD.
Methods A total of 374 patients with CKD were enrolled. Serum samples were collected, and the levels of soluble (P)RR and prorenin were measured using ELISA kits. Serum creatinine (Cr), blood urea nitrogen (BUN), uric acid (UA), hemoglobin (Hb), soluble secreted α-Klotho, and the urine protein/Cr ratio were also measured. Similarly, clinical parameters were also evaluated using serum and urine sample collected after 1 year ($n = 204$).
Results Soluble (P)RR levels were positively associated with serum Cr ($P < 0.0001$, $r = 0.263$), BUN ($P < 0.0001$, $r = 0.267$), UA ($P < 0.005$, $r = 0.168$) levels, CKD stage ($P < 0.0001$, $r = 0.311$) and urine protein/Cr ratio ($P < 0.01$, $r = 0.157$), and inversely with estimated glomerular infiltration rate (eGFR) ($P < 0.0001$, $r = -0.275$) and Hb ($P < 0.005$, $r = -0.156$). Soluble (P)RR levels were inversely associated with α-Klotho levels ($P < 0.001$, $r = -0.174$) but did not correlate with prorenin levels. With respect to antihypertensive drugs, soluble (P)RR levels were significantly lower in patients treated with an angiotensin II receptor blocker (ARB) than in those without ARB therapy ($P < 0.005$). Soluble (P)RR levels were significantly lower in CKD patients with diabetes mellitus or primary hypertension than in those without these conditions ($P < 0.05$). In contrast, serum levels of prorenin did not correlate with parameters related to renal function. Serum prorenin levels were significantly higher in CKD patients with diabetes mellitus than in nondiabetic patients ($P < 0.05$), but not in CKD patients with hypertension ($P = 0.09$). Finally, with respect to the relationship between basal soluble (P)RR levels and the progression rates of renal function, soluble (P)RR levels were positively associated with ΔCr ($P < 0.05$, $r = 0.159$) and inversely associated with ΔeGFR ($P < 0.05$, $r = -0.148$).
Conclusion Serum levels of soluble (P)RR correlated with the stage of CKD. Our findings suggest that soluble (P)RR may be involved in renal injury and influence the progression of CKD.

Keywords Prorenin · Soluble (pro)renin receptor · Chronic kidney disease

K. Hamada · Y. Taniguchi · Y. Shimamura · K. Inoue · K. Ogata · M. Ishihara · T. Horino · S. Fujimoto · Y. Terada (✉)
Department of Endocrinology, Metabolism and Nephrology, Kochi University School of Medicine, Kohasu, Oko-cho, Nankoku, Kochi 783-8505, Japan
e-mail: terada@kochi-u.ac.jp

T. Ohguro · Y. Yoshimoto
Department of Internal Medicine, Kochi Red Cross Hospital, Kochi, Japan

M. Ikebe · K. Yuasa
Department of Urology and Internal Medicine, Kochi-Takasu Hospital, Kochi, Japan

E. Hoshino · T. Iiyama
Clinical Trial Center, Kochi University School of Medicine, Kochi, Japan

A. Ichihara
Department of Endocrinology and Hypertension, Tokyo Women's Medical University, Tokyo, Japan